

Chemical vapor deposition of sp^2 -boron nitride on Si(111) substrates from triethylboron and ammonia: effect of surface treatments

Running title: CVD of sp^2 -BN on Si(111)

Running Authors: Souqui et al.

Laurent Souqui, Henrik Pedersen, Hans Högberg ^{a)}

Department of Physics, Chemistry and Biology (IFM), Linköping University, SE-581 83,
Linköping, Sweden.

^{a)} Electronic mail: hans.hogberg@liu.se

Thin films of the sp^2 -hybridized polytypes of boron nitride are interesting materials for several electronic applications such as UV-devices. Deposition of epitaxial sp^2 -BN films has been demonstrated on several technologically important semiconductor substrates such as SiC and Al_2O_3 and where controlled thin film growth on Si would be beneficial for integration of sp^2 -BN in many electronic device systems. We

investigate growth of BN films on Si(111) by chemical vapor deposition from triethylboron $B(C_2H_5)_3$ and ammonia NH_3 at 1300 °C with focus on treatments of the Si(111) surface by nitridation, carbidization and nitridation followed by carbidization prior to BN growth. Fourier transform infrared spectroscopy shows that the BN films deposited exhibit sp^2 bonding. X-ray diffraction reveals that the sp^2 -BN films predominantly grow amorphous on untreated and pre-treated Si(111), but with diffraction data showing that turbostratic BN can be deposited on Si(111) when the formation of Si_3N_4 is avoided. We accomplish this condition by a nitridation procedure in a deposition chamber where B_xC had previously been deposited at high temperature, but where the synthesis route needs to be further developed for a better process control.

I. INTRODUCTION

The sp^2 -hybridized forms of boron nitride (sp^2 -BN), hexagonal and rhombohedral boron nitrides (h-BN¹ and r-BN²) are promising thin film materials for applications in *e.g.* UV-devices³⁻⁵, neutron detectors⁵⁻⁷ and graphene electronics⁸⁻¹⁰. Epitaxial growth of sp^2 -BN by chemical vapor deposition (CVD) has been demonstrated on 3C-SiC(111), 4H- and 6H-SiC(0001) on-axis substrates and α - Al_2O_3 (0001) at temperatures above 1200 °C¹¹⁻¹⁵. However, these substrates require surface pre-treatment to support nucleation of BN, where controlled graphitization¹⁶ or ramping up in a SiH_4 - H_2 ambient¹³ was needed on SiC substrates while controlled nitridation to form AlN supported growth on α - Al_2O_3 (0001) substrates^{11,17}.

As silicon forms the backbone in microelectronics it would be favorable to integrate sp^2 -BN films in silicon technology. This endeavor requires development of a

deposition process for epitaxial growth at temperatures below the melting point of silicon at 1414 °C as well as consideration of the higher chemical reactivity of silicon compared to SiC and Al₂O₃. The literature reveals several studies to deposit sp²-BN on silicon substrates by thermal CVD. Depositions performed below 1000 °C on Si, with several boron precursors such as diborane (B₂H₆)^{18–23}, decaborane(14) (B₁₀H₁₄)²⁴, triethylboron (TEB, B(C₂H₅)₃)²⁵ and ammonia (NH₃) or with single-source precursors such as ammonia-borane (H₃NBH₃)¹⁰ and B-trichloroborazine (B₃Cl₃N₃H₃)²⁶ resulted in growth of amorphous BN. Turbostratic BN (t-BN) films was reported at 800 °C from borazine (B₃N₃H₆)²⁷, at 980 °C from N-trimethyl borazine (B₃H₃N₃(CH₃)₃)²⁸ and at 1200 °C using TEB²⁵ or BCl₃²⁹. Polycrystalline films were deposited from B₂H₆ and NH₃ at 1200 °C on Si(100)¹⁹ and nanocrystalline films from TEB and NH₃ on Si(111) at 1350 °C⁵. Comparing to growth on SiC and α-Al₂O₃, the need for surface pre-treatment of Si substrates is still an open question and therefore a suitable subject for investigation.

In this study, we investigate a thermal CVD route for deposition of sp²-BN films on Si(111) using TEB and NH₃, focusing on pre-treatment of the Si(111) surface to improve nucleation condition and favor the growth of crystalline sp²-BN. The Si(111) surface is modified by exposure to either TEB or NH₃, forming an interlayer on which BN films are deposited by CVD at 1300 °C.

II. EXPERIMENTAL DETAILS

A. *Film deposition*

The BN films were deposited by CVD at 1300 °C during 60 min from TEB, (semiconductor grade quality, from SAFC Hitech) and NH₃ (99.999 %, further

purified by a getter filter to reduce the water content) on pre-treated Si(111) substrates, as described below, in a horizontal hot-wall reactor equipped with TaC-coated graphite susceptor held at base pressure below 9×10^{-7} mbar. All films were deposited with a NH_3/TEB ratio of 321 (0.3 sccm TEB) and at a process pressure of 70 mbar. In addition, silane (SiH_4 , 99.999 % purity, 2000 ppm diluted in 99.9996 % H_2) was supplied with a flow corresponding to 0.005 sccm pure SiH_4 , during growth following previous results on r-BN films deposited at 1500 °C.³⁰ Prior to insertion in the reaction cell the Si(111) substrates were degreased and etched *ex-situ* using acetone and ethanol, 5 min each, in an ultrasonic bath at 80 °C and then immersed in HF solution (2 %).

Prior to BN growth, the cleaned Si(111) surface was exposed *in-situ* to different substrate pretreatments in the CVD reactor: nitridation, carbidization, nitridation followed by carbidization, and no pre-treatment, meaning stabilization of the temperature of the Si(111) substrate in a H_2 ambient. Pre-treatments of the Si(111) substrates were conducted as follows:

Nitridation by stabilizing the temperature at 1050 °C in 3000 sccm H_2 for 25 min, then heating up to 1300 °C and holding for 5 min with addition of 0.005 sccm SiH_4 , followed by 90 sccm NH_3 and 0.009 sccm SiH_4 for 120 min.

Carbidization by stabilizing the temperature at 1050 °C in 3000 sccm H_2 for 25 min, then heating up to 1300 °C and holding for 5 min with addition of 0.009 sccm SiH_4 , followed by 0.28 sccm TEB and 0.009 sccm SiH_4 for 3 s.

Nitridation followed by carbidization by stabilizing the temperature at 1050 °C in 3000 sccm H_2 for 25 min, then heating up to 1300 °C and holding for 5 min with addition of 0.005 sccm SiH_4 , then exposing the Si(111) surface to 90 sccm NH_3

and 0.009 sccm SiH₄ for 120 min followed by a 3 s exposure to 0.009 sccm SiH₄ and 0.28 sccm TEB.

No pretreatment meant that the substrates were only maintained in 3000 sccm H₂ for 25 min at 1050 °C then heated up to 1300 °C and held for 5 min with 0.005 sccm SiH₄ directly followed by BN deposition.

To study a potential “boron memory” effect in the deposition chamber for the growth of BN, rhombohedral boron carbide (r-B_xC) coatings were deposited on to saturate the deposition chamber with boron prior to the deposition of BN on Si(111). 4H-SiC(0001) substrates were used for characterization of the coatings. The B_xC was deposited at 1500°C and 70 mbar using 5000 sccm H₂ and 0.7 sccm TEB diluted in 150 sccm H₂ in a separate quartz liner.

B. Film characterization

Fourier transform infrared spectroscopy (FTIR) reflectance spectra were measured in a Bruker VERTEX 70 equipment with incident s-polarized light at an angle of 60° with respect to the sample surface normal. The spectra were acquired at room temperature, after a 30 min N₂ purge, with 2 cm⁻¹ resolution and averaged over 50 scans. A thin film of gold was used as reference. The FTIR peaks were fitted using a Lorentzian profile and linear base line using SciDAVis software (version 1.22).

X-ray diffraction (XRD) was used to investigate the phase distribution and film orientation. All diffractograms were recorded using Cu K α radiation (Cu K β removed by a nickel filter). The 2 θ / ω diffractograms were recorded in a PANalytical X'Pert Pro diffractometer with a Bragg-Brentano HD and 1/2° slit as primary optics and X'celerator detector with a 5 mm anti scatter slit on the secondary side. The

diffractograms in grazing-incidence diffraction (GID) configuration, ϕ -scans and pole figures were recorded in a Phillips X'Pert MPD diffractometer with crossed slits ($2 \times 2 \text{ mm}^2$) and $1/2^\circ$ slit as primary optics and proportional detector (PW1711/96) equipped with parallel plate collimator on the secondary side.

Plane view scanning electron micrographs were obtained by operating the microscope (LEO 1550 Gemini) at 5 kV with an in-lens secondary electron microscope.

III. RESULTS AND DISCUSSION

A. Vibrational spectroscopy

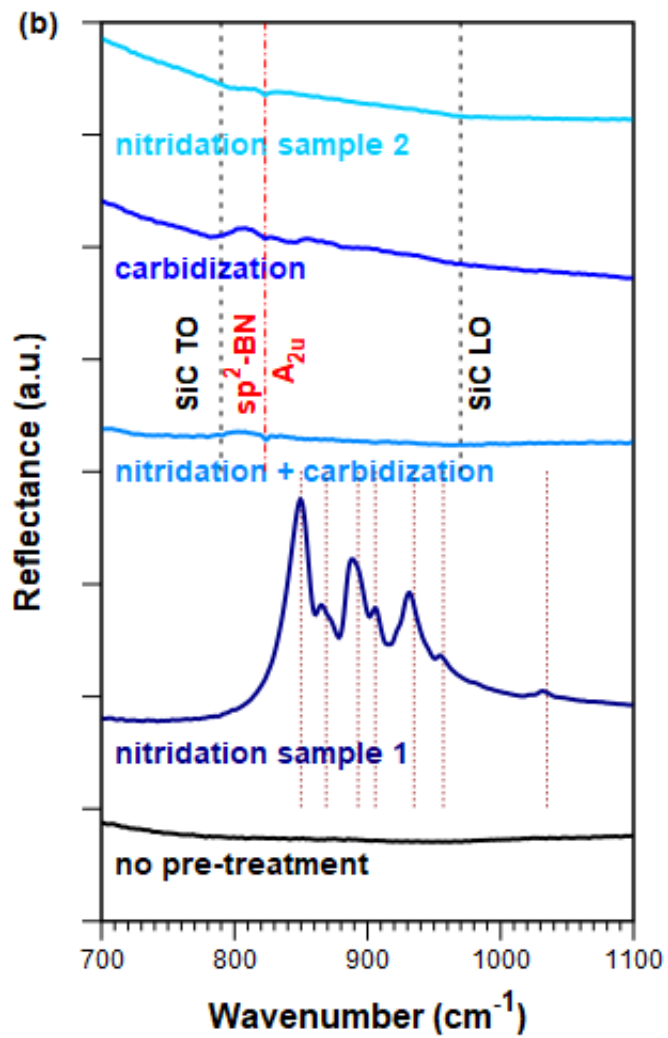
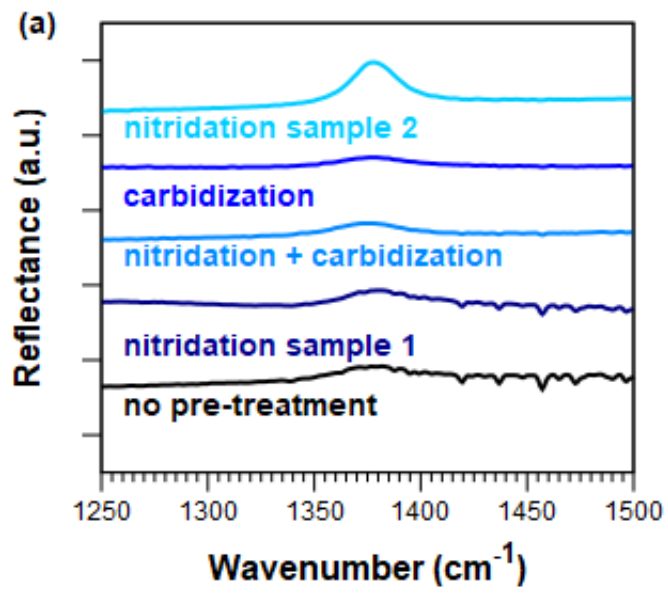


FIG. 1. FTIR reflectance spectra recorded from BN films deposited on Si(111) substrates either without pre-treatment or with nitridation using 2 different samples, carbidization, and initial nitridation followed by carbidization, showing in (a) the wavenumber range 1250 and 1500 cm^{-1} around the $E_{1u}(\text{TO})$ mode of sp^2 -BN and in (b) the wavenumber range 700 and 1000 cm^{-1} around the $A_{2u}(\text{TO})$ mode of sp^2 -BN (red dotted dashed line). In (b) the black dotted lines at 796 cm^{-1} and at 973 cm^{-1} represent the TO and LO bands of SiC, respectively³¹ and where wine-colored dotted lines show reflectance peaks from crystalline Si_3N_4 ^{32,33}.

FTIR was applied to characterize the chemical bonding structure of the BN films deposited on the Si(111) substrate without pre-treatment or on Si(111) substrates with different pre-treatments, see Figure 1. As can be seen in Figure 1a spectra recorded around the in-plane stretching, transverse optical (TO) $E_{1u}(\text{TO})$ mode for sp^2 -BN³⁴⁻³⁷ show broad peaks of low intensities centered around 1377 cm^{-1} , but where one spectrum measured from a BN film deposited on a Si(111) substrate pre-treated by nitridation displays a more visible peak given a higher reflectance, see the reflectance curve at the top in Figure 1a. Thus, the spectra show that the BN films deposited exhibit sp^2 bonding. For the former group of spectra, the measured full width at half maximum (FWHM) values of $E_{1u}(\text{TO})$ peak were similar seen from $38.0 \pm 1.3 \text{ cm}^{-1}$, but with a lower FMWH of 25.7 cm^{-1} for the BN film with the reflectance peak of highest intensity. We note that the determined FWHM value for this film in FTIR is comparable to a FWHM of 25 cm^{-1} reported from measurement of the E_{2g} Raman stretching mode at 1366 cm^{-1} of a nanocrystalline BN film deposited on Si(111)^{1,5} Figure 1b shows spectra measured around the out-of-plane bending, longitudinal optical (LO) $A_{2u}(\text{LO})$ mode at 823 cm^{-1} for sp^2 -BN³⁴⁻³⁷. In the figure

only two peaks originating from sp^2 -BN are discernable and marked by a red dotted dashed line. These peaks are only visible on BN films deposited on substrates pre-treated by carbidization or nitridation followed by carbidization. This supports the results from Figure 1a that sp^2 -BN nucleates on some of the pre-treated Si(111) substrates.

Furthermore, Figure 1b shows the formation of crystalline Si_3N_4 on a Si(111) substrate pre-treated by nitridation seen from the sharp reflection bands in the wavenumber range 850 to 960 cm^{-1} ^{32,33} that are marked by wine-colored dotted lines. The formation of crystalline Si_3N_4 will be supported from thin film XRD below. It is important to note that the sample displaying the sharp peak related to sp^2 -BN in Figure 1a does not display any peaks related to Si_3N_4 as encountered in Figure 1b. Visible in Figure 1 b and for the sample pre-treated by carbidization are the Reststrahlen bands of silicon carbide (SiC) with the TO band at 796 cm^{-1} and the LO at 973 cm^{-1} ³¹. The full spectra, in unit of reflectance, are shown in Figure S1 in the supporting info.

B. X-ray diffraction

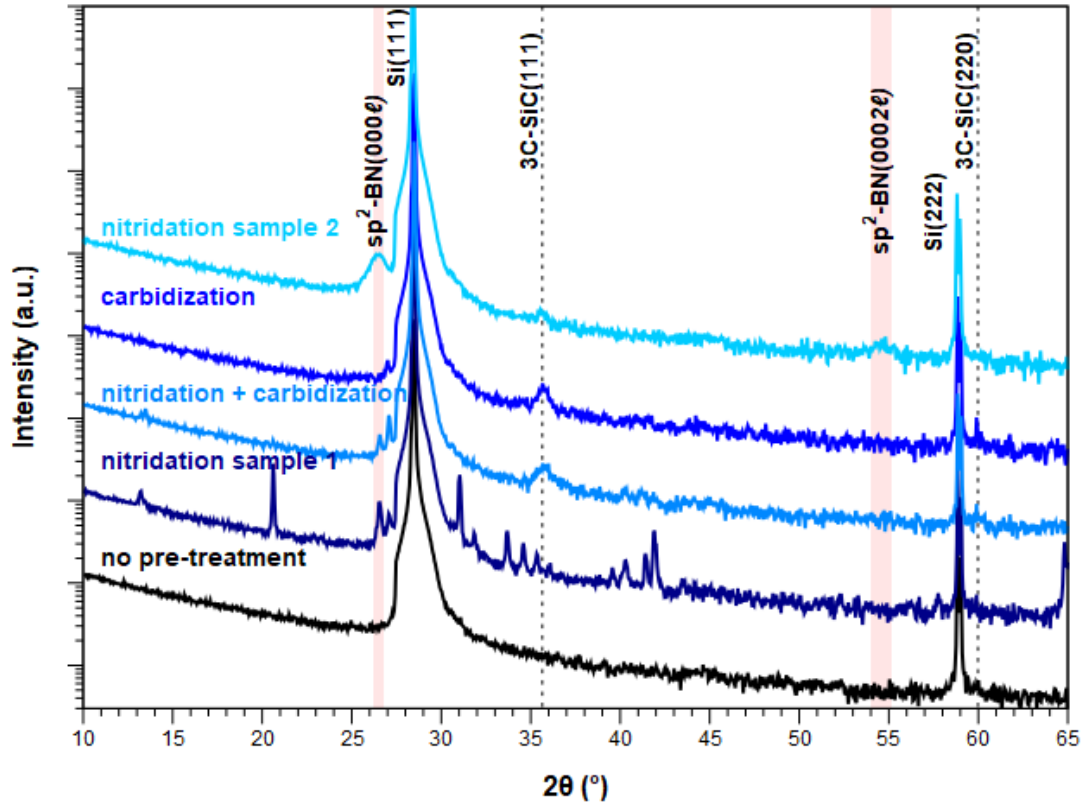


FIG. 2. $2\theta/\omega$ diffractograms of BN films deposited from TEB and NH_3 at 1300°C and 70 mbar in H_2 on Si(111) substrates either without pre-treatment or with nitridation using 2 different samples, carbidization, and initial nitridation followed by carbidization. The sharp peaks observed around the reported values for $sp^2\text{-BN}(000\ell)$ (shaded areas) correspond to $\alpha\text{-Si}_3\text{N}_4(20\bar{2}0)$, $2\theta = 26.5^\circ$ and $\beta\text{-Si}_3\text{N}_4(20\bar{2}0)$, $2\theta = 26.9^\circ$. The dotted lines indicate reflections from SiC.

The phase distribution for the deposited BN films was investigated by X-ray $2\theta/\omega$ scans, see Figure 2. In the diffractograms no peaks related to crystalline $sp^2\text{-BN}$ are encountered for films deposited on either the un-treated or any of the pre-treated Si(111) substrates. Instead several sharp peaks related to crystalline Si_3N_4 and 3C-SiC

are visible in the diffractograms. See the supporting information for more details on the structural properties of the formed Si_3N_4 and SiC (Figure S3 and S4). Thus, XRD suggests that the sp^2 -BN detected by FTIR is amorphous on $\text{Si}(111)$ without pre-treatment, on Si_3N_4 and 3C-SiC as well on $\text{Si}(111)$ pre-treated by nitridation followed by carbidization. In contrast, the sample displaying a sharper sp^2 -BN $E_{1u}(\text{TO})$ absorption peak in FTIR shows a diffractogram with 2 peaks originating from sp^2 -BN at $2\theta = 26.5^\circ$ and at $2\theta = 54.4^\circ$. The broad, low intensity peaks are the 000ℓ and 0002ℓ peaks from sp^2 -BN. In addition, the 111 peak from 3C-SiC is visible in diffractograms, see Figure 2 and S2. Pole figure measurement were conducted for the $r\text{-BN}\{01\bar{1}2\}$ planes $h\text{-BN}\{10\bar{1}2\}$ planes, see Figure 3a and 3b, respectively. No poles or ring originating from $r\text{-BN}$ at $\psi = 66^\circ$ or for $h\text{-BN}$ at $\psi = 56^\circ$ were detected in the pole figures, see red dashed lines in Figure 3a and 3b. This suggests that the film is $t\text{-BN}$.³⁸ In contrast to the other samples, the diffractogram recorded from the sample with the highest quality sp^2 -BN does not display any diffraction peaks originating from crystalline Si_3N_4 , which is supported by the FTIR results, see Figure 1b. This observation will be further developed in section D.

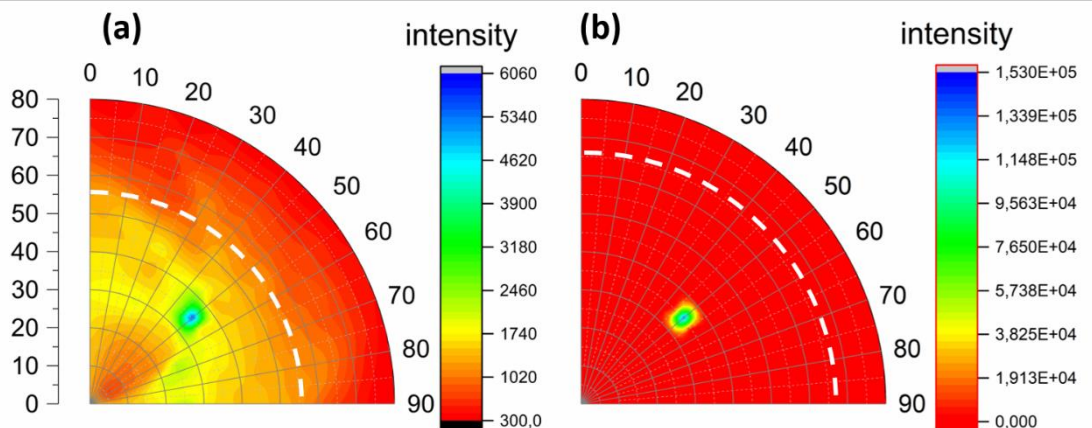


FIG. 3. Pole figure measurements for (a) $h\text{-BN}\{10\bar{1}2\}$ planes (43.874°) and (b) $r\text{-BN}\{01\bar{1}2\}$ planes (45.566°). Only a quarter of the pole figure was measured to allow

longer measurement times. The red dashed segment of rings are guides for the eyes indicating the ψ value where the poles from for h-BN in (a) at $\psi = 56^\circ$ and r-BN in (b) at $\psi = 66^\circ$ are expected. The strong sharp pole at around 35° originates from Si{220} planes ($2\theta = 47.305^\circ$).

From the 2θ angle of the 000ℓ at 26.5° it was possible to calculate the interplanar distance ($d_{000\ell}$) in the deposited film to $d_{000\ell} = 3.37 \text{ \AA}$. This value is larger than that for bulk h- and r-BN with $d_{000\ell} = 3.33 \text{ \AA}$, where the higher interplanar distance supports the formation of t-BN³⁹⁻⁴². The determined distance $d_{000\ell} = 3.37 \text{ \AA}$ is larger than the value reported for films deposited from B_2H_6 ¹⁹ and BCl_3 ²⁹ at 1200°C ($d_{000\ell} = 3.34 \text{ \AA}$). It is, however, closer to that of h- and r-BN than the value $d_{000\ell} = 3.5 \text{ \AA}$ previously determined for as-deposited t-BN films grown from borazine at 900°C ²⁷ and from TEB and NH_3 at 1200°C ²⁵. In addition, XRD shows that our t-BN films are textured with the c-axis parallel to Si[111] as evident by the absence of t-BN(10 $\bar{1}$ 0) and t-BN(11 $\bar{2}$ 0) in $2\theta/\omega$ diffractogram whereas the films deposited from B_2H_6 ¹⁹ and BCl_3 ²⁹ are randomly oriented.

C. *Surface morphology*

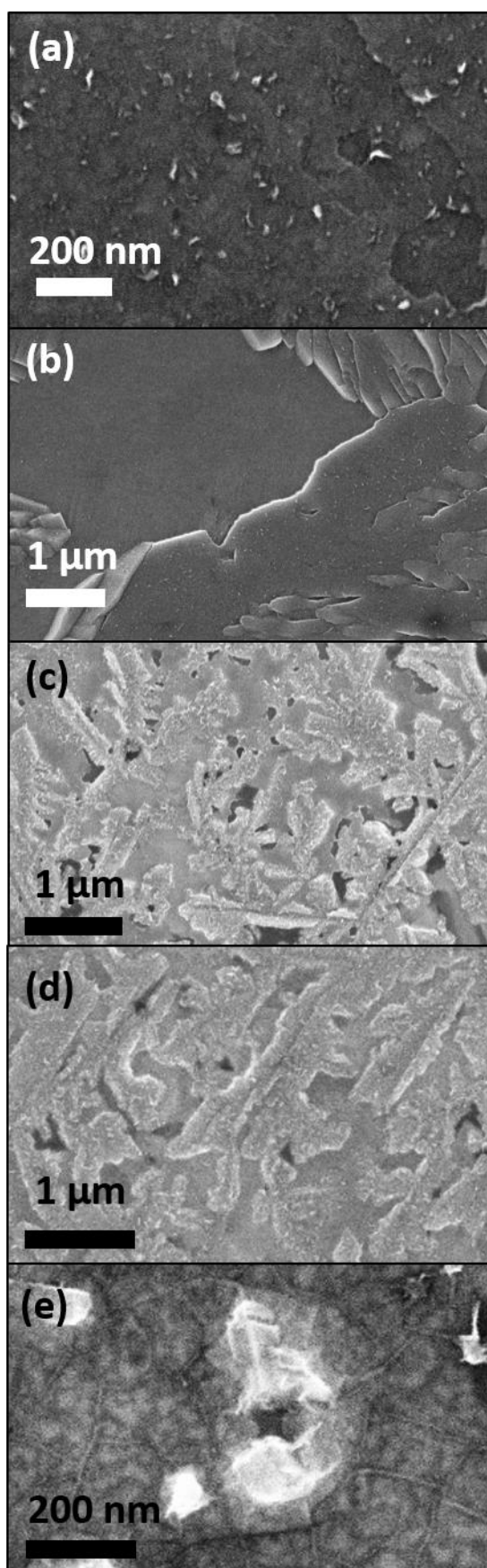


FIG. 4. Plane-view SEM images from: (a) a BN film deposited directly on Si(111), (b) a BN film deposited after nitridation of the Si(111) surface (nitridation sample 1), (c) a BN film deposited after nitridation and carbidization of the Si(111) surface, (d) a BN film deposited after carbidization of the Si(111) surface, and (e) a BN film deposited after nitridation of the Si(111) surface (nitridation sample 2) corresponding to film with peaks related to sp^2 -BN in the diffractogram in Figure 2.

The amorphous sp^2 -BN films presented a fibrous to dendritic surface morphology as visible from the plan-view scanning electron microscopy (SEM) images in Figure 4a, b, c, and d. A fibrous surface morphology is similar to that previously observed in epitaxial growth of r-BN on $Al_2O_3(0001)$ substrates following nitridation⁴³. From the images, we note that the films deposited on the untreated and nitridated surfaces in Figure 4a and b displayed a lower island nucleation density compared to the carbidized surfaces in Figure 4c and d. This difference in nucleation rate on Si_3N_4 and SiC is supported by the lower intensity of both modes of BN in FTIR for BN deposited on nitridized Si(111) in Figure 1. We suggest that part of the ammonia is consumed to grow Si_3N_4 instead of BN, even after 120 min surface nitridation. In addition, the nitridation pre-treatment results in a coarsening of the Si(111) surface seen from randomly oriented silicon nitride grains in the order of 10 μm in size (Figure 4b and S5). It should be noted that a few isolated Si_3N_4 crystals were found on the non-pretreated Si(111) surface, following deposition of BN. The carbidized surface showed a dendritic surface morphology (Figure 4(c and d) and S6). Etch pits are observed for both nitridation and carbidization (Figure 4(b-d), S5 and

S6), which is likely an indication of Si atoms originating from the substrate that form a nitride and a carbide, respectively.

Figure 4e shows the morphology of the film exhibiting the FTIR and XRD peaks from t-BN. In the image flat t-BN grains about 200-nm in size with visible grain boundaries are evident on the sample surface together with coarse SiC grains as well as amorphous sp^2 -BN with fibrous morphology. The morphology of sp^2 -BN in these films differs from the often reported pebble-like morphology in sp^2 -BN films from borazine and BCl_3 .^{27,29} We suggest that this is due to the difference in chemistry, as the MOCVD process involves a significant amount of C while both halide- and borazine-based processes are essentially free from C. Our films were stable in ambient air for more than 24 months. Hence, the degradation process reported by Pedersen et al.²⁵ for BN films deposited on Si(111) substrates in the temperature range 800 to 1200 °C was not observed in any of our deposited films. A possible explanation for a higher stability is the higher deposition temperature of 1300 °C applied in our study that should favor the growth of less porous film. This is supported by the smaller interplanar distance determined by XRD.

D. Boron memory-effect-induced growth of BN

As previously determined from XRD, occasionally nitridation of the Si(111) substrate promoted the deposition of t-BN films with a higher crystalline quality. This was supported from FTIR by peaks originating from sp^2 -BN as well as from SEM revealing a surface morphology containing clearly visible sp^2 -BN grains. A common property of these samples was the absence of peaks related to Si_3N_4 when investigated by FTIR and XRD. These observations could not be explained by a solid-state

reaction of Si_3N_4 after exposure to TEB to form BN and SiC, as pre-treatment by nitridation and subsequent carbidization by a flow of TEB show similar results as pre-treatment by direct carbidization. Our pre-treatment experiments conducted show that the formation of crystalline Si_3N_4 is favored both in nitridation and carbidization as well as irreversible seen from pre-treatment by nitridation followed by carbidization. this is supported by XRD and FTIR spectra, showing that NH_3 was consumed without reaction with the Si surface in order to form BN.

Here, we speculate that a surface covered by B could result in the formation of a passivating BN layer on the Si(111) surface prior to the nitridation. This type of surface condition could prevent the formation of Si_3N_4 and allow for the nucleation of crystalline sp^2 -BN. To test this hypothesis, we introduced for typically applied process conditions a relatively large amount of B into the reactor and conducted deposition of boron carbide (B_xC) from dissociation of TEB at 1500 °C during 120 min, using 4H-SiC(0001) as substrates as a consequence of the choice of deposition temperature. The phase distribution and chemical bonding in the resulting r- B_xC films were characterized by XRD and FTIR, see Figures S7 and S8, respectively. Following the dummy deposition, the reactor was cooled down and the 4H-SiC substrates coated with r- B_xC films were replaced by Si(111) substrates. The substrates were heated to 1300 °C and then exposed to SiH_4 during 15 min, which was followed and by nitridation during 120 min. Note that the pre-treatment by nitridation was not followed by a CVD process for growth of BN from TEB and NH_3 , but that a BN film was formed just by exposing the Si substrates to NH_3 as shown by the $2\theta/\omega$ diffractograms shown in Figure 5. These diffractograms from BN films deposited with and without SiH_4 present during the nitridation, shows that the addition of SiH_4 results in a more distinct BN peak.

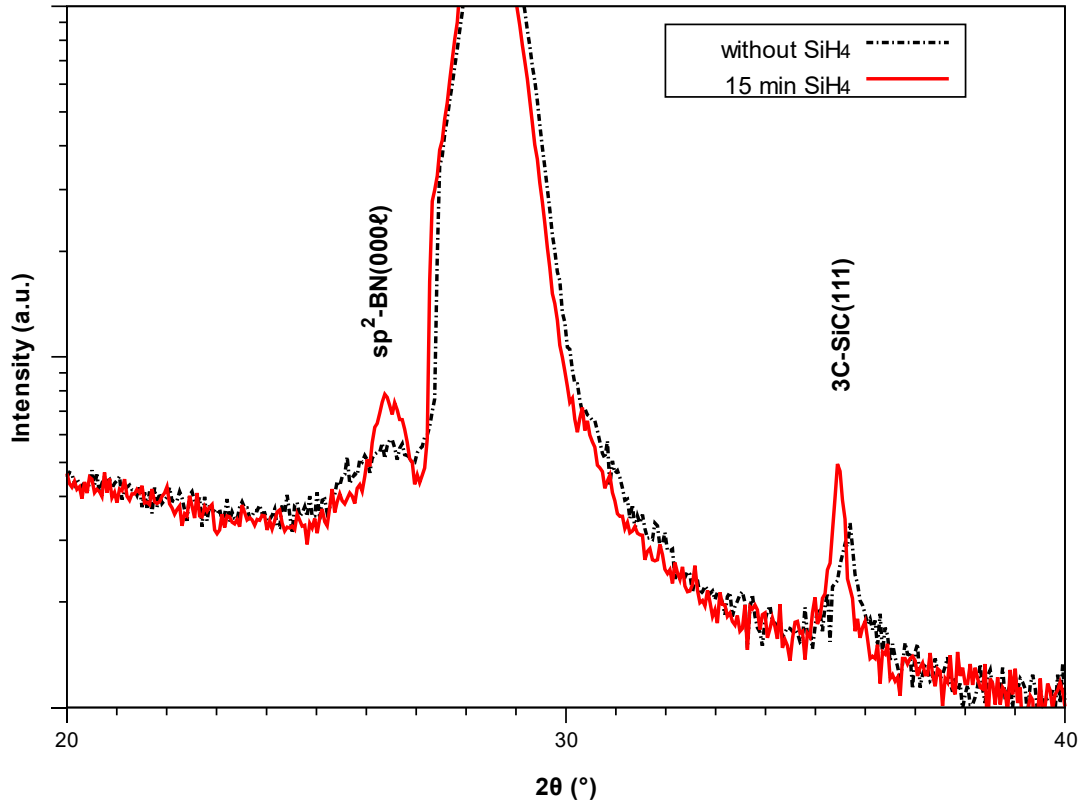


FIG. 5. $2\theta/\omega$ diffractograms of BN films deposited at 1300 °C and by nitridation of the Si(111) substrate at 1300 °C with and without exposure to SiH₄ prior to nitridation in a CVD reactor previously saturated with B from the dissociation of TEB at 1500 °C during by 120 minutes.

Figure 6 shows the surface morphology of the BN film deposited following dissociation of TEB and nitridation. In the figure, the darker flat grains are from sp²-BN, while the bright faceted grains are from 3C-SiC and with no trace of grains from Si₃N₄. The surface structure of the BN film is to a large extent similar to those previously described for the crystalline sp²-BN films deposited on nitridated Si(111) where Si₃N₄ did not form, but with larger sp²-BN grains surrounding the SiC grains. In addition, from Figure 6, we note the absence of fibrous amorphous sp²-BN on the SiC grains previously described in Figure 4c. The fact that TEB was not introduced in

the chamber suggests that B_xC acts as boron source in growth of sp^2 -BN films on the Si(111) substrates.

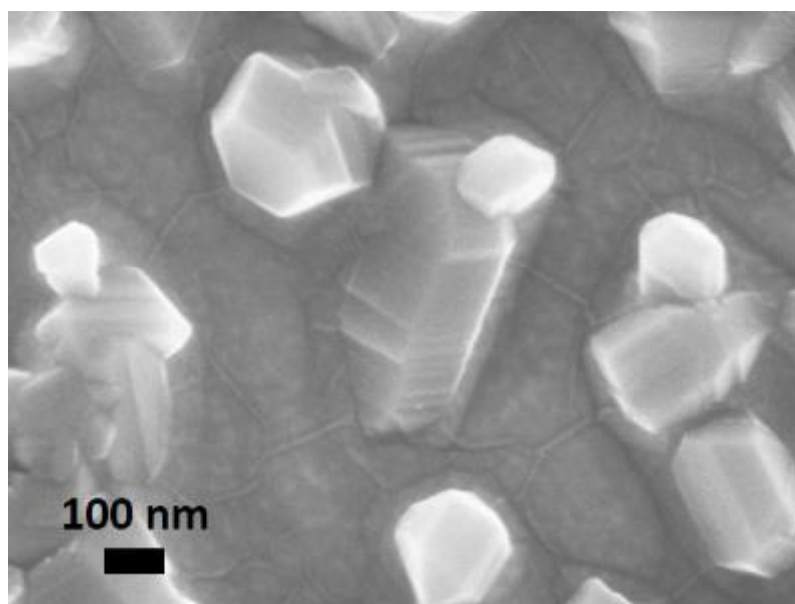


FIG. 6. Plane-view SEM image of a BN film deposited in the CVD reactor following dissociation of TEB at 1500 °C for 120 minutes and nitridation at 1300 °C.

It also suggests that the 15 min exposure to SiH_4 and H_2 was sufficient to promote growth of sp^2 -BN to cover the silicon surface thereby preventing the formation of Si_3N_4 . This was further investigated by exposing a $r-B_xC/4H-SiC$ dummy to hydrogen and silane for 15 minutes. The concentration of each gases was the same as for the previous BN deposition without TEB. As can be seen from Figure 7a, the $r-B_xC$ facets display a smooth surface. Following exposure to the hydrogen-silane gas mixture the surface structure of the $r-B_xC$ facets changes and where 50-nm-wide etch pits becomes visible on faceted grains, see Figure 7b. This suggests that $r-B_xC$ reacts with H_2 or SiH_4 to form volatile B-containing and possibly additional C-containing species. The presence of such species in the gas phase may account for the possibility of depositing BN without boron precursor.

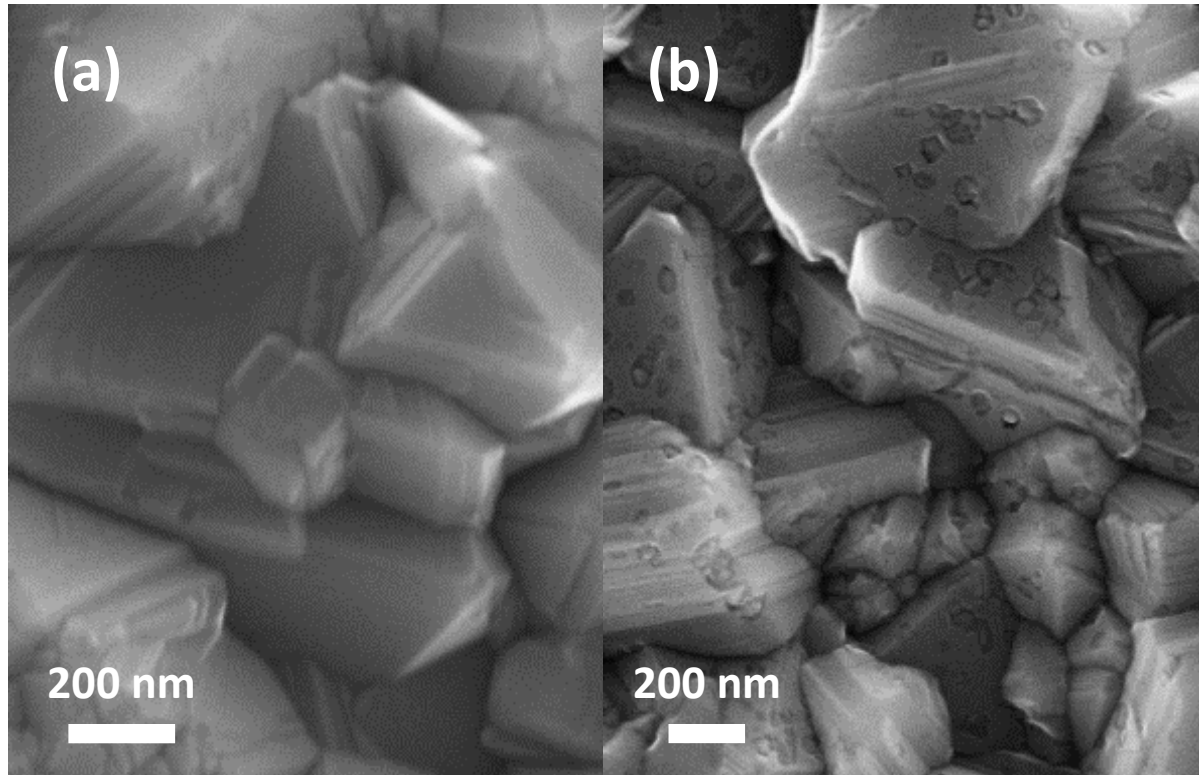


FIG. 7. In (a), plane-view SEM image of a B_xC film deposited on SiC at 1500 °C using 0.7 sccm TEB and 5000 sccm H_2 for 120 min. In (b), plane-view SEM image of the surface in (a) following exposure to 0.005 sccm SiH_4 and 3000 sccm H_2 at 1300 °C for 15 min.

IV. CONCLUSIONS

We investigate CVD of boron nitride from $B(C_2H_5)_3$ TEB and NH_3 on Si(111) at 1300 °C where the substrate surface is pre-treated by nitridation, carbidization and nitridation followed by carbidization prior to BN growth. XRD shows that BN grow amorphous when deposited directly on the Si(111) surface and after nitridation of the Si(111) substrate. SEM images reveal that the nucleation density for amorphous sp^2 -BN on crystalline 3C-SiC is higher compared to un-treated and Si(111) pre-treated by nitridation. Exposing the nitridated surface to TEB results in continued growth of

amorphous sp^2 -BN and the formation of crystalline 3C-SiC but with Si_3N_4 grains present on the surface. This supports the stability of Si_3N_4 as the formation of SiC did not promote the growth of crystalline BN.

In addition, we find that t-BN with a degree of crystalline order can be deposited on Si using the nitridation pre-treatment, as shown by XRD and FTIR. We show that this can be accomplished by depositing a r- B_xC coating on the chamber walls and then utilizing r- B_xC as boron precursor to form t-BN on Si(111) from the reaction with NH_3 .

ACKNOWLEDGMENTS

This work was supported by the Swedish Foundation for Strategic Research (SSF) and contract IS14-0027. H.P. and H.H. acknowledge the financial support from the Swedish Government Strategic Research Area in Materials Science on Advanced Functional Materials at Linköping University (Faculty Grant SFO-Mat-LiU no. 2009-00971).

References

- ¹ R.S. Pease, *Acta Crystallogr.* **5**, 356 (1952).
- ² T. Sato, *Proc. Japan Acad.* **61**, 459 (1985).
- ³ K. Watanabe, T. Taniguchi, and H. Kanda, *Nat. Mater.* **3**, 404 (2004).
- ⁴ Y. Kubota, K. Watanabe, O. Tsuda, and T. Taniguchi, *Science* **317**, 932 (2007).
- ⁵ K. Ahmed, R. Dahal, A. Weltz, J.Q. Lu, Y. Danon, and I.B. Bhat, *Appl. Phys. Lett.* **109**, 113501 (2016).

- ⁶ T.C. Doan, A. Marty, J. Li, J.Y. Lin, and H.X. Jiang, in *Proc. SPIE* (2016), p. 99680S.
- ⁷ A. Maity, T.C. Doan, J. Li, J.Y. Lin, and H.X. Jiang, *Appl. Phys. Lett.* **109**, 072101 (2016).
- ⁸ E. Kim, T. Yu, E. Sang Song, and B. Yu, *Appl. Phys. Lett.* **98**, 262103 (2011).
- ⁹ W. Gannett, W. Regan, K. Watanabe, T. Taniguchi, M.F. Crommie, and A. Zettl, *Appl. Phys. Lett.* **98**, 242105 (2011).
- ¹⁰ M.S. Bresnehan, M.J. Hollander, M. Wetherington, K. Wang, T. Miyagi, G. Pastir, D.W. Snyder, J.J. Gengler, A.A. Voevodin, W.C. Mitchel, and J.A. Robinson, *J. Mater. Res.* **29**, 459 (2014).
- ¹¹ M. Chubarov, H. Pedersen, H. Högberg, V. Darakchieva, J. Jensen, P.O.Å. Persson, and A. Henry, *Phys. Status Solidi - Rapid Res. Lett.* **5**, 397 (2011).
- ¹² M. Chubarov, H. Pedersen, H. Högberg, J. Jensen, and A. Henry, *Cryst. Growth Des.* **12**, 3215 (2012).
- ¹³ M. Chubarov, H. Pedersen, H. Högberg, Z. Czigany, and A. Henry, *CrystEngComm* **16**, 5430 (2014).
- ¹⁴ N. Umehara, A. Masuda, T. Shimizu, I. Kuwahara, and T. Kouno, *Jpn. J. Appl. Phys.* **55**, 05FD09 (2016).
- ¹⁵ L. Souqui, H. Pedersen, and H. Högberg, *J. Vac. Sci. Technol. A* **37**, 020603 (2019).
- ¹⁶ Y. Kobayashi, H. Hibino, T. Nakamura, T. Akasaka, T. Makimoto, and N. Matsumoto, *Jpn. J. Appl. Phys.* **46**, 2554 (2007).
- ¹⁷ K. Ahmed, R. Dahal, A. Weltz, J.J.Q. Lu, Y. Danon, and I.B. Bhat, *Mater. Res. Express* **4**, 015007 (2017).
- ¹⁸ M.J. Rand and J.F. Roberts, *J. Electrochem. Soc.* **115**, 423 (1968).

- ¹⁹ M. Hirayama and K. Shohno, *J. Electrochem. Soc.* **122**, 1671 (1975).
- ²⁰ S.P. Murarka, C.C. Chang, D.N.K. Wang, and T. E. Smith, *J. Electrochem. Soc.* **126**, 1951 (1979).
- ²¹ A.C. Adams and C.D. Capio, *J. Electrochem. Soc.* **127**, 399 (1980).
- ²² K. Shohno, T. Kim, and C. Kim, *J. Electrochem. Soc.* **127**, 1546 (1980).
- ²³ A. Essafti, C. Gomez-Aleixandre, and J. Albella, *Vacuum* **45**, 1029 (1994).
- ²⁴ K. Nakamura, *J. Electrochem. Soc.* **132**, 6 (1982).
- ²⁵ H. Pedersen, M. Chubarov, H. Högberg, J. Jensen, and A. Henry, *Thin Solid Films* **520**, 5889 (2012).
- ²⁶ R. Stolle and G. Wahl, in *J. Phys. IV* (1995), pp. C5-761-C5-768.
- ²⁷ J.-S. Li, C.-R. Zhang, B. Li, F. Cao, and S.-Q. Wang, *Surf. Coat. Technol.* **205**, 3736 (2011).
- ²⁸ Y. Ye, U. Graupner, and R. Krüger, *Chem. Vap. Depos.* **18**, 249 (2012).
- ²⁹ P. Carminati, T. Buffeteau, N. Daugey, G. Chollon, F. Rebillat, and S. Jacques, *Thin Solid Films* **664**, 106 (2018).
- ³⁰ M. Chubarov, H. Pedersen, H. Högberg, and A. Henry, *CrystEngComm* **15**, 455 (2013).
- ³¹ D. Olego and M. Cardona, *Phys. Rev. B* **25**, 1151 (1982).
- ³² N. Wada, S.A. Solin, J. Wong, and S. Prochazka, *J. Non. Cryst. Solids* **43**, 7 (1981).
- ³³ J.P. Luongo, *J. Electrochem. Soc.* **130**, 1560 (1983).
- ³⁴ R. Geick, C. Perry, and G. Rupprecht, *Phys. Rev.* **146**, 543 (1966).
- ³⁵ P.J. Gielisse, S.S. Mitra, J.N. Plendl, R.D. Griffis, L.C. Mansur, R. Marshall, and E.A. Pascoe, *Phys. Rev.* **155**, 1039 (1967).
- ³⁶ D.M. Hoffman, G.L. Doll, and P.C. Eklund, *Phys. Rev. B* **30**, 1 (1984).
- ³⁷ A. Soltani, P. Thévenin, and A. Bath, *Diam. Relat. Mater.* **3**, 831 (1994).

- ³⁸ M. Chubarov, H. Högberg, A. Henry, and H. Pedersen, *J. Vac. Sci. Technol. A Vacuum, Surfaces, Film.* **36**, 030801 (2018).
- ³⁹ W. Ruland, *Acta Crystallogr.* **18**, 992 (1965).
- ⁴⁰ Y. Hishiyama and M. Nakamura, *Carbon N. Y.* **33**, 1399 (1995).
- ⁴¹ H. Fujimoto, *Carbon N. Y.* **41**, 1585 (2003).
- ⁴² Z.Q. Li, C.J. Lu, Z.P. Xia, Y. Zhou, and Z. Luo, *Carbon N. Y.* **45**, 1686 (2007).
- ⁴³ M. Chubarov, H. Pedersen, H. Högberg, S. Filippov, J.A.A. Engelbrecht, J. O'Connell, and A. Henry, *Phys. B Condens. Matter* **439**, 29 (2014).